




A Prospective Outlook on the Development of Exoskeletal Knee Joints for Prostheses via a Design Concept Evaluation Approach

Muhammad Farzik Ijaz^{1,2,*} , Abdulhamid A. Al-Abduljabbar^{1,2}, Khalid Alluhydan¹, Meshari Aloraini¹, Reyhan Alajlan¹ and Khalid Almuahaya¹

¹Mechanical Engineering Department, College of Engineering, King Saud University, Riyadh, Saudi Arabia
²King Salman Center for Disability Research, Riyadh, Saudi Arabia

Correspondence to:
Muhammad Farzik Ijaz*, e-mail: mijaz@ksu.edu.sa; farzik98@gmail.com

Received: 29 January 2023; Revised: 1 May 2023; Accepted: 9 May 2023; Published Online: 30 May 2023

ABSTRACT

Disability is a complex multidimensional challenge and it can substantially limit the major life activities of a person. In the Kingdom of Saudi Arabia, it is estimated that 3.73% of the population have functional disabilities. People with disability always stay in the same posture which limits their social independence. A brief introduction and a literature review about exoskeletal prostheses and a preliminary analysis of the biomechanics of passive knees are presented in this paper. The proposed knee joint design has key features that are similar to other currently available knee joints for prosthetic legs. The main components of our design include single-axis knee joints, legs, and sockets. We limited our investigation to a handful of biomechanical variables that can be easily evaluated and generate some targets for long-term rehabilitation research. Thus, by following the cognitive principle of engineering design methodology, i.e. the “weight and rate criterion,” we provide a preliminary concept and theoretical calculations for the development of a cost-effective knee joint system. The Ansys engineering simulation and three-dimensional design software such as SOLIDWORKS simulation were utilized to provide an outlook of our initial prototype. In addition, by subjective and objective approaches, from our theoretical calculation for our designed product, the factor of safety was determined to be higher than 1.5.

KEYWORDS

exoskeletal implant, preliminary study, theoretical calculations, factor of safety

INTRODUCTION

The loss of a body part has been witnessed from the beginning of the ages in humans, and this happens due to several reasons including diseases, accidents, and wars, and the cost of an artificial implant is very high at the moment for some members in the community. In injured patients, the lack of mobility for a long time can cause several medical and psychological issues. Patients around the world are now requiring implants that can last longer and provide less discomfort but at a reduced cost. The most comprehensive study found was the “Disability Survey 2017” report published by the General Authority for Statistics (GASat) of Saudi Arabia in 2017. The GASat surveyed a random sample of 33,575 households in a way that guarantees representation nationwide in 2017 to determine the demographics of people with physical and intellectual disability across Saudi Arabia [Putti, 1930; Miller, 1946; Engstrom and Van de Ven 1999; Ebnezar, 2000; Andrysek, 2010; May and Lockard 2011;

Bindawas and Vennu, 2018]. According to the report, 1.6% of people in Saudi Arabia have extreme locomotor disability. Few studies have been published on the demographics of amputees in Saudi Arabia. Nowadays many artificial lower limbs are available on the market, and each one of them uses different mechanisms and materials, and the main factor between these artificial limbs is the mechanism of the knee joint, which are summarized in Table 1. Human movement is a biomechanically efficient process. A healthy person may travel vast distances while consuming little energy. Despite advancements in prosthetic design, replacing lower-limb segments with a prosthesis reduces mobility efficiency. The goal of a lower-limb prosthesis is to reduce the impact of the amputation and restore the patient’s independence. Hence, the prosthesis technology focuses on simulating the joint behavior of human lower limbs when walking. Therefore, understanding the gait cycle and the resulting mechanical

Table 1: Summary of the different types of knee joints available on the market.

Name	Specifications	Type	Cost
LIMBS Knee [Narang 2013] 	<ul style="list-style-type: none"> • Light weight • No advance technology • Short-life material • Low stability 	Four bar	\$20 75 SR
The 802 Nylon Knee [Arelekatti 2015] 	<ul style="list-style-type: none"> • Light weight • No advance technology • Handle weight up to 100 kg • Low maintenance and durability 	Single axis Hydraulic	\$2100 7875 SR
C-leg [Kannenberg 2014] 	<ul style="list-style-type: none"> • Highly stable • Advance technology • Handle weight up to 130 kg • Batteries live up 45 hours for one charge 	Single axis Microprocessor hydraulic	\$54,500 204,375 SR
Genium [Farina and Aszmann 2014] 	<ul style="list-style-type: none"> • Light weight • Advance technology • Handle weight up to 150 kg • Batteries live up 120 hours for one charge 	Single axis Microprocessor hydraulic	\$75,000 281,250 SR

forces that impact the whole cycle is crucial for designing exoskeletal devices. For people with transfemoral amputations, prosthetic knees are cutting-edge medical devices that use mechanical mechanisms and components to imitate the natural biological knee function [Preuss, 1911; American Academy of Orthopaedic Surgeons, 1960; Fliegel and Feuer, 1966; Padula and Friedmann, 1987; Hibbeler 1994; Shigley et al., 2004; Lambrecht 2008; Narang, 2013; Rodriguez-Merchan 2013; Bergmann et al., 2014; Kannenberg et al., 2014; Arelekatti, 2015; Pirker and Katzenschlager 2017]. By presenting a biomechanical overview of prosthetic knees, this article seeks to fill in this knowledge gap.

METHODS

This study presents an outlook on the designing of knee-related passive implants. The research methodology is subdivided into various categories. A schematic diagram explicitly indicating the outline of the sequence of steps that are followed for executing the present study is shown

in Figure 1. In this paper, the salient results revealing the design of a knee implant according to durable biomechanical requirements are discussed. Furthermore, theoretical calculation encompassing the various structural components is also included. Also, we present ideas about three general trends in the current and future development of prosthetic knees in terms of the design project approach.

RESULTS AND DISCUSSION

Equilibrium analysis and theoretical design calculations

For our study, we defined the maximum body weight as 100 kg. From the literature it is known that the maximum force acting on the knee during walking (gait cycle 55%, knee flexion angle 20°) is around $F_z = -3571$ N. This shows that the forces on the other direction are very small compared to the force on the z direction as summarized in Table 2. In order to find out the amount of forces acting on the device,

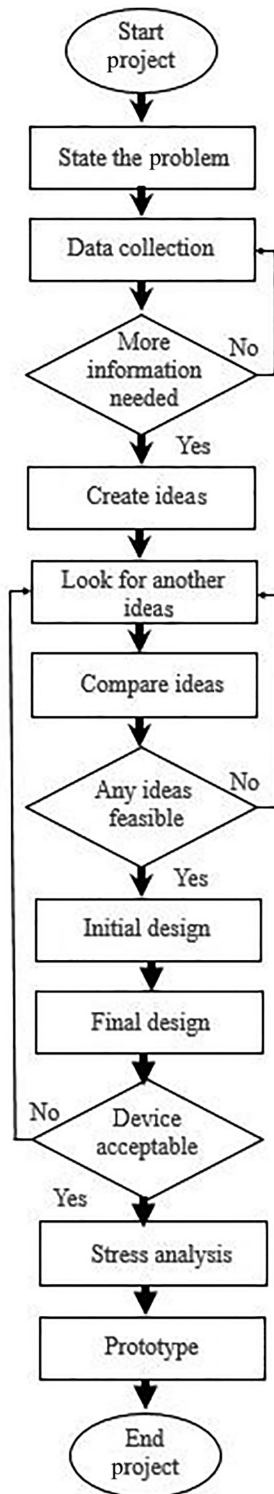


Figure 1: Flow chart showing the sequence of steps involved in the present design project.

we divided the external load by 2, one for each side of the knee, and the free body diagram (FBD) of each section is presented in Figures 2-6, respectively.

$$F_z = \frac{3571}{2} = 1785.5 \text{ N}$$

From FBD-1:

$$\sum F_z = 0$$

$$F_{Lz} = F_z = 1785.5 \text{ N}$$

$$\sum M_y \text{ at Point } L = 0$$

$$M_L = F_z \times \left(\frac{4.32}{1000} \right)$$

From FBD-2:

$$\sum M_y \text{ at Point } A = 0$$

$$F_{Springz} \times \frac{57}{1000} + M_{plate} = F_z \times \frac{21.17}{1000}$$

$$\sum F_z = 0$$

$$F_z = F_{Springz} + F_{platez}$$

From FBD-3:

$$\sum M_y \text{ at Point } A = 0$$

$$M_{plate} = F_{platez} \times \frac{12.7}{1000}$$

From FBD-4:

$$\sum F_x = 0$$

$$F_{platex} = 0$$

Figures 7 and 8 summarize the force versus displacement and moment versus displacement charts, respectively.

Here, at the middle of the bar, we will have the critical point:

$$T_{max} = 18.340 \text{ kN} - \text{mm}, M_{max} = 33.42735 \text{ kN} - \text{mm}$$

From the literature it is known that the load fluctuates from nearly 0 N to a maximum of 3571 N; so, we assumed that the force is between 0 load and 3571 N (repeated stress) to continue further analysis.

Table 2: Summary of loads acting on knees and their equilibrium reactions.

Type of load	Forces					Moments	
Unit	Newton					Newton-meter	
Name	F_z	F_{Lz}	F_{plateX}	F_{platez}	$F_{Springz}$	M_L	M_{plate}
Value for one side	1785.5	1785.5	0	1444	341.4	7.713	18.34
Total value	3571	3571	0	1444	682.8	15.426	18.34

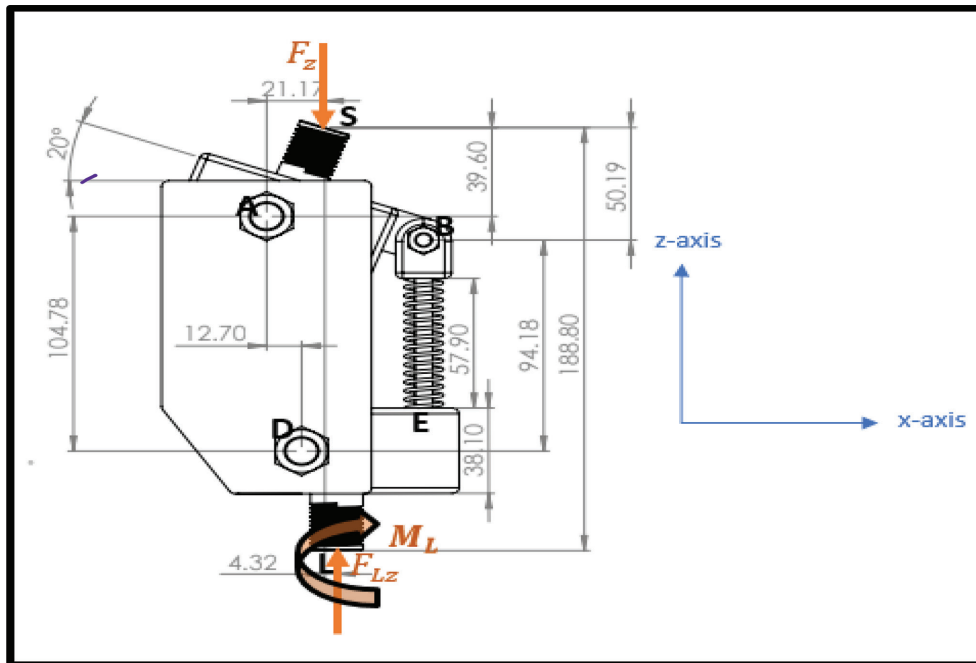


Figure 2: FBD-1 for the knee section. Abbreviation: FBD, free body diagram.

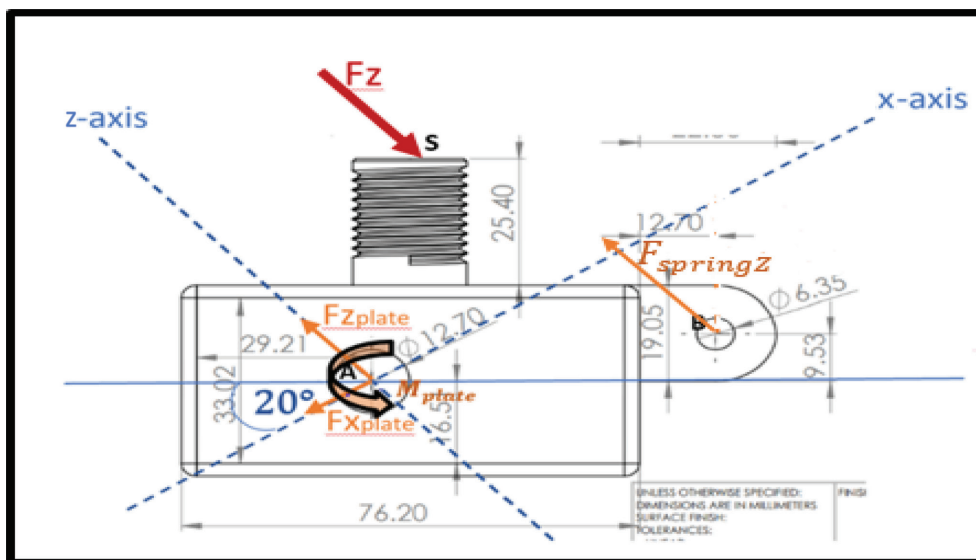


Figure 3: FBD-2 for the upper connector section. Abbreviation: FBD, free body diagram.

For the bar material, we chose 1030 hot rolled steel, which has the following specifications [Ijaz et al., 2016]:

$$S_{ut} = 470 \text{ MPa}, S_y = 260 \text{ MPa}$$

We have no change in cross sections; therefore, we assume that any stress concentration factor = 0.

Endurance limit S_e calculations:

$$d = 12 \text{ mm}$$

$$I = \frac{\pi}{64} \times d^4 = \frac{\pi}{64} \times \frac{12^4}{1000^4} = 1.018 \times 10^{-9} \text{ m}^4$$

$$J = \frac{\pi}{2} r^4 = 2.035 \times 10^{-9} \text{ m}^4$$

$$\text{Non-rotating : } d_e = 0.37d = 0.37 \times 12 = 4.44 \text{ mm}$$

$$K_b = 1.24 d^{-0.107} = 1.24 \times 12^{-0.107} = 1.057$$

$$K_a = a S_{ut}^b = 4.51 \times 290^{-0.265} = 1.004$$

$$K_c = K_d = K_e = k_f = 1$$

$$S'_e = 0.5S_{ut} = 0.5 \times 470 = 235 \text{ MPa}$$

$$S_e = S'_e K_a K_b K_c K_d K_e K_f = 249.38 \text{ MPa}$$

Stress calculations:

$$\sigma_{min} = 0$$

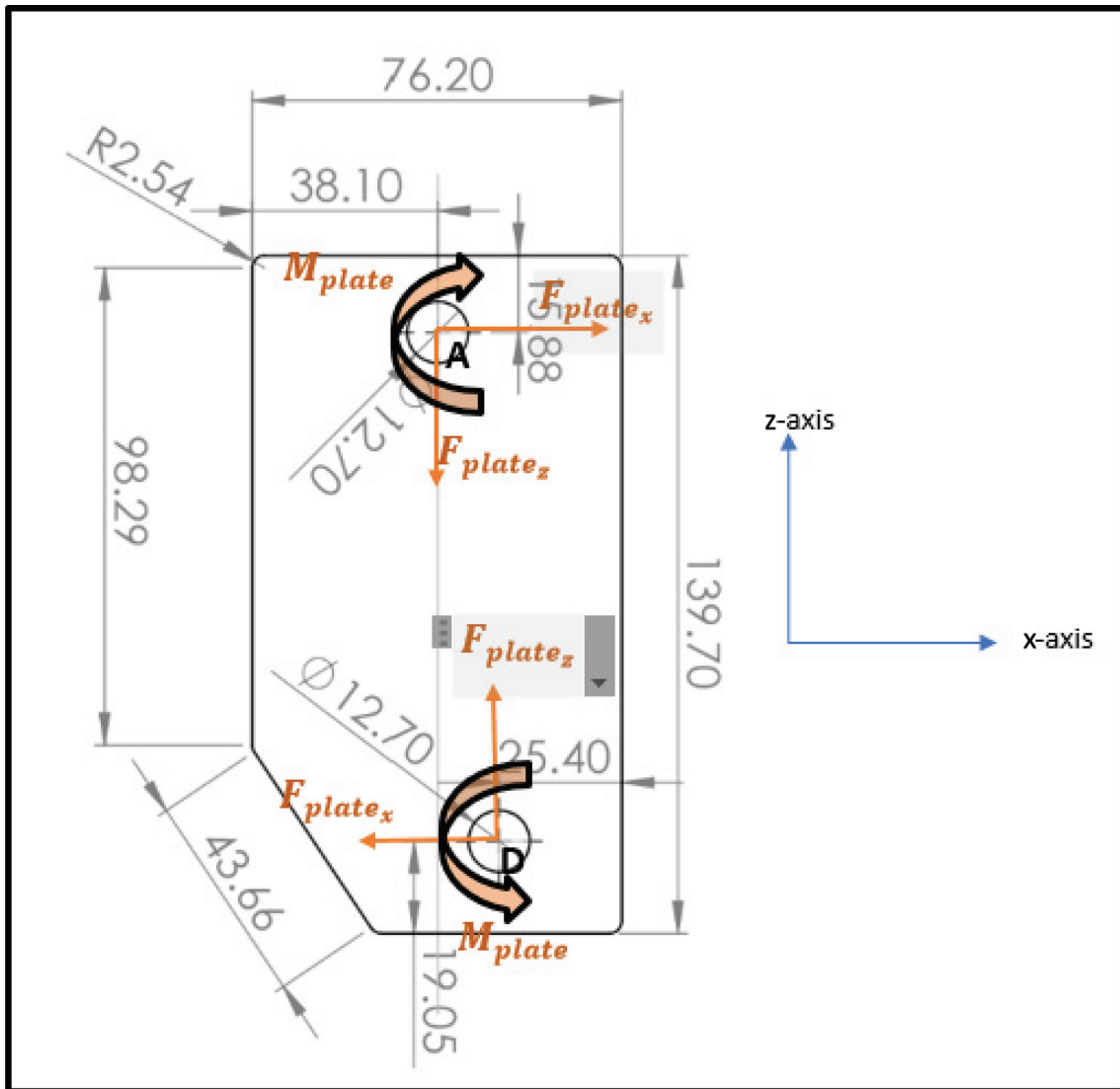


Figure 4: FBD-3 for the plate section. Abbreviation: FBD, free body diagram.

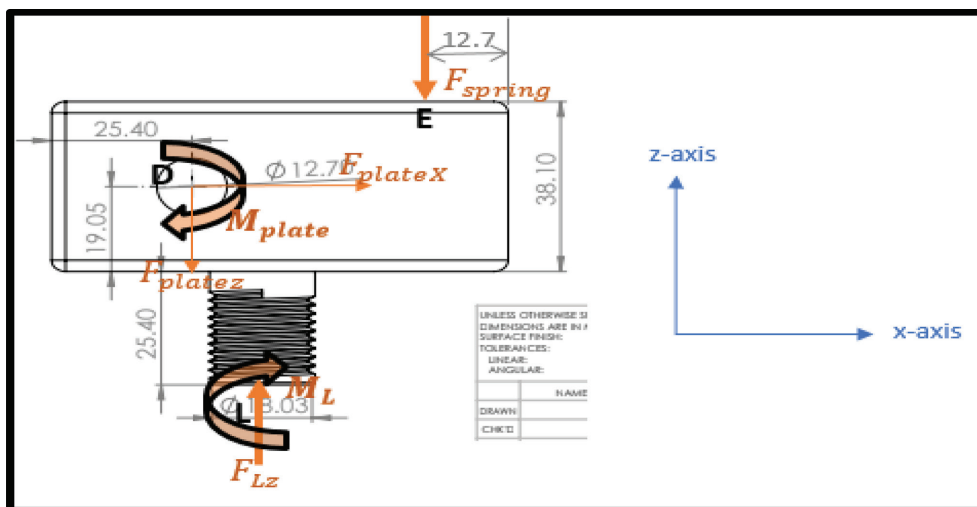


Figure 5: FBD-4 for the lower connector section. Abbreviation: FBD, free body diagram.

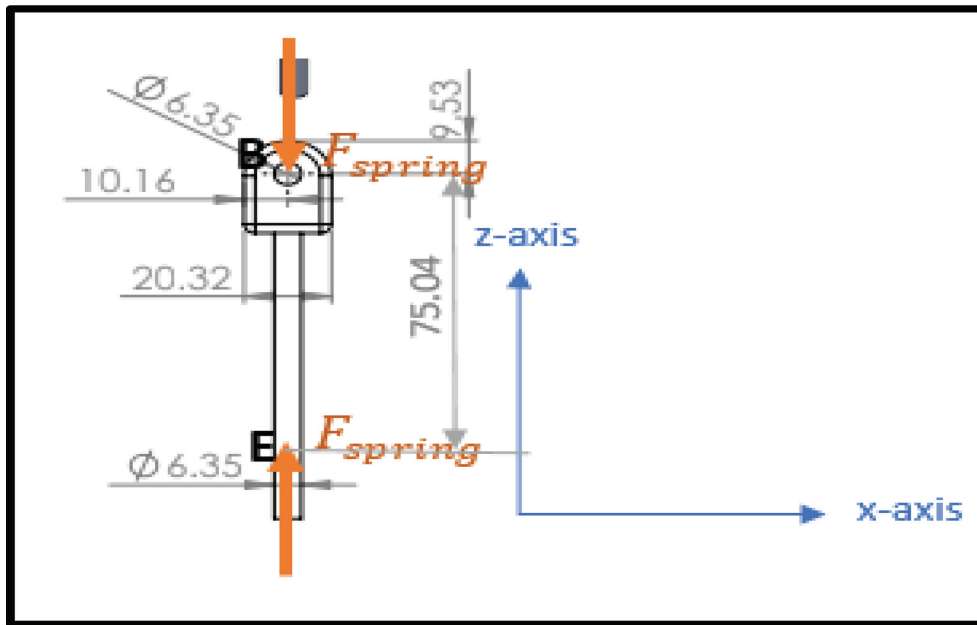


Figure 6: FBD-5 for the spring connector section. Abbreviation: FBD, free body diagram.

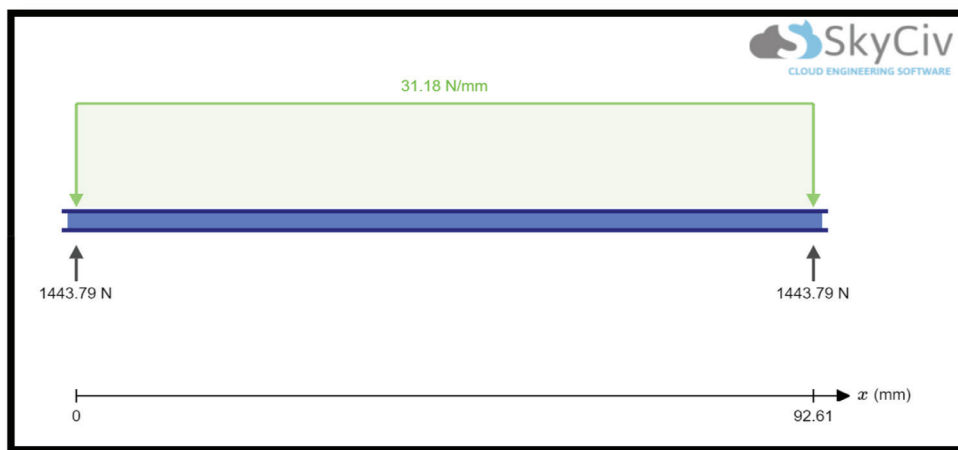


Figure 7: Force vs. displacement chart.

$$\sigma_{max} = \frac{M_{max}c}{I} = \frac{33.42735 \times \frac{6}{1000}}{1.018 \times 10^{-9}} = 196.98 \text{ MPa}$$

$$\tau_{max} = \frac{T_{max}c}{J} = \frac{18.34 \times \frac{6}{1000}}{2.035 \times 10^{-9}} = 54.07 \text{ MPa}$$

$$\sigma'_{max} = \sqrt{(\sigma_{max})^2 + 3(\tau_{max})^2} = (218.1096) \text{ MPa}$$

$$\sigma'_a = \frac{\sigma'_{max}}{2} = 109.05 \text{ MPa}$$

$$\sigma'_m = \frac{\sigma'_{max}}{2} = 109.05 \text{ MPa}$$

$$\text{Fatigue factor of safety } n_f : \frac{1}{n_f} = \frac{\sigma'_a}{S_e} + \frac{\sigma'_m}{S_{ut}} \rightarrow n_f = 1.59 > 1$$

$$\text{Static factor of safety } n_y : n_y = \frac{S_y}{\sigma'_a + \sigma'_m} = 2.19 > 1$$

Endurance limit calculation for the rod used for constructing the leg

For the leg rod material, we chose Al-6061 rolled, which has the following specifications [Ijaz et al., 2016]:

$$S_{ut} = 290 \text{ MPa}, S_y = 255 \text{ MPa}$$

We have no change in cross sections; therefore, we assume that any stress concentration factor = 0.

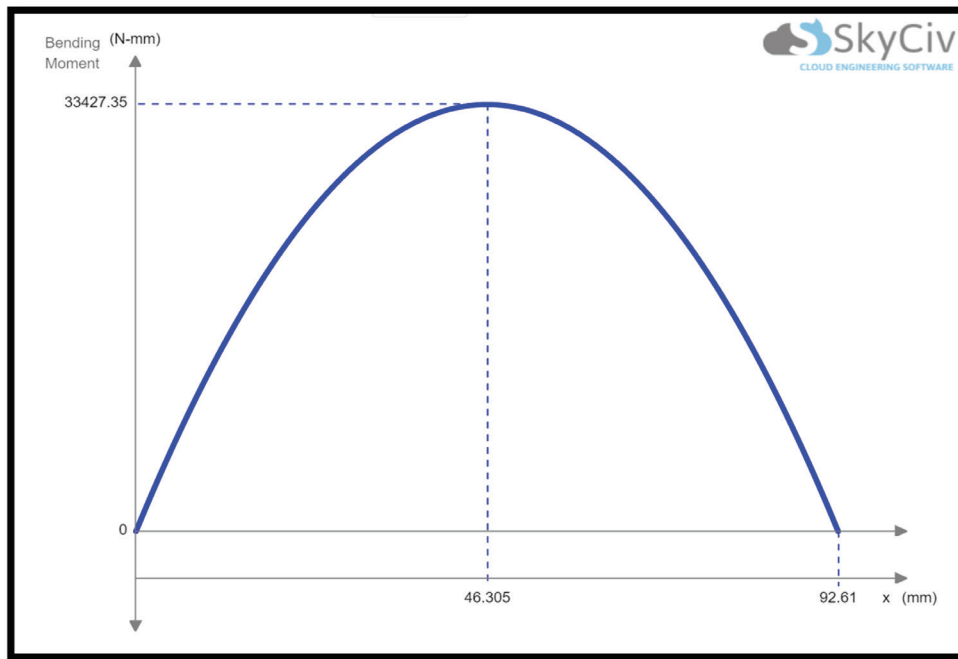


Figure 8: Moment vs. displacement chart.

Endurance limit S_e calculations:

For aluminum Al-T6061:

$$\sigma_y = 255 \text{ MPa}; E = 68.9 \text{ GPa}$$

For the rod:

$$D = 0.0281 \text{ m}; L = 0.4318 \text{ m}; K = 1$$

Effective length factor:

$$L_e = K \times L = 0.4318 \text{ m}$$

The moments of inertia for the leg:

$$I = \frac{\pi}{64} (0.0281^4 - 0.01905^4) = 2.41 \times 10^{-8} \text{ m}^4$$

The area of the cross section:

$$A = \frac{\pi}{4} (0.0281^2 - 0.01905^2) = 3.35 \times 10^{-4} \text{ m}^2$$

Non-rotating: $d_e = 0.37d = 0.37 \times 0.0381 = 0.0141 \text{ m}$

$$K_b = 1.24 d^{-0.107} = 1.24 \times 14.1^{-0.107} = 0.93$$

$$K_a = a S_{ut}^b = 4.51 \times 290^{-0.265} = 1.004$$

$$K_c = K_d = K_e = k_f = 1$$

$$S'_e = 0.5 S_{ut} = 0.5 \times 290 = 145 \text{ MPa}$$

$$S_e = S'_e K_a K_b K_c K_d K_e K_f = 136 \text{ MPa}$$

$$\sigma_{min} = 0$$

$$M_L = M_{max} = 15.426 \text{ MPa}$$

$$\sigma_{max} = \frac{M_{max} c}{I} + \frac{F_{Lz}}{A} = \frac{15.426 \times \frac{19.05}{1000}}{2.41 \times 10^{-8}} + \frac{3571}{3.35 \times 10^{-4}} = 19.65 \text{ MPa}$$

$$\sigma'_{max} = \sqrt{(\sigma_{max})^2 + 3(\tau_{max})^2} = 19.65 \text{ MPa}$$

$$\sigma'_a = \frac{\sigma'_{max}}{2} = 9.83 \text{ MPa}$$

$$\sigma'_m = \frac{\sigma'_{max}}{2} = 9.83 \text{ MPa}$$

$$\text{Fatigue factor of safety } n_f: \frac{1}{n_f} = \frac{\sigma'_a}{S_e} + \frac{\sigma'_m}{S_{ut}} \rightarrow n_f = 9.42 > 1$$

$$\text{Static factor of safety } n_y: n_y = \frac{S_y}{\sigma'_a + \sigma'_m} = 12.97 > 1$$

Buckling analysis of prosthetic pylon tubes

Buckling is considered as the common mode of failure in the prosthetic pylon tube materials such as aluminum Al-T6061 [27].

$$\sigma_y = 255 \text{ MPa}; E = 68.9 \text{ GPa}$$

For the rod:

$$D = 0.0281 \text{ m}; L = 0.4318 \text{ m}; K = 1$$

Effective length factor:

$$L_e = K \times L = 0.4318 \text{ m}$$

The moments of inertia for the leg:

$$I = \frac{\pi}{64} (0.0281^4 - 0.01905^4) = 2.41 \times 10^{-8} \text{ m}^4$$

The area of the cross section:

$$A = \frac{\pi}{4} (0.0281^2 - 0.01905^2) = 3.35 \times 10^{-4} \text{ m}^2$$

Euler's formula:

$$P_{cr} = \frac{\pi^2 E I}{L_e^2} = \frac{\pi^2 \times 68.9 \times 10^9 \times 2.41 \times 10^{-8}}{0.4318^2} = 87896.32 \text{ N}$$

$$\sigma_{cr} = \frac{P_{cr}}{A} = \frac{87896.32}{3.35 \times 10^{-4}} = 262.38 \text{ MPa}$$

$$\sigma_{allow} = \left[212 - 1.59 \left(\frac{KL}{r} \right) \right] = 131.03 \text{ MPa}$$

$$\sigma_{allow} \langle \sigma_{cr} \quad ; \quad n = 2.2 \rangle 1$$

Static analyses of helical spring design

In this section, we will cover the design approach for the helical spring; there is a systematic method of designing starting with the number of constraints:

The preferred range of the spring index is $4 \leq C \leq 12$, with the lower indexes being more difficult to form (due to the risk of surface cracking) and springs with higher indexes tending to tangle often enough to require individual packing. This can be the first item for the design assessment. The recommended range of active turns is $3 \leq N_a \leq 15$. To maintain linearity, when a spring is about to close, it is necessary to avoid the gradual touching of coils (due to no perfect pitch). The rest of the constraints are stated below [Ijaz et al., 2016]:

$$D = d_{rod} + d + allow$$

$$4 \leq C \leq 12$$

$$3 \leq N_a \leq 15$$

$$\xi \geq 0.15$$

$$n_s \geq 1.2$$

Design assumptions

After a number of iterations, the best design dimensions are stated below:

$$d = 2 \text{ mm}$$

$$D = 8.55 \text{ mm}$$

$$N_a = 15 \text{ coils}$$

$$L_o = 58 \text{ mm}$$

After determining the primary dimensions, we performed the spring design calculations using the following equations:

$$C = \frac{D}{d} = 4.275$$

$$K_B = \frac{4C + 2}{4C - 3} = 1.354$$

$$\tau_s = \frac{8K_B(1 + \xi)F_{max} \cdot D}{(\pi d)^3} = 293.17 \text{ MPa}$$

A helical compression spring is made of no. 30 music wire.

$$S_{ut} = \frac{A}{d^m} = \frac{2211}{2^{0.145}} = 1999.58 \text{ MPa}$$

$$S_{sy} = 0.45S_{ut} = 0.45(1999.58) = 899.81 \text{ MPa}$$

$$\text{Factor of safety } n_s = \frac{S_{sy}}{\tau_s} = 3.069$$

$$OD = D + d = 10.55 \text{ mm}$$

$$ID = D - d = 6.55 \text{ mm}$$

$$N_a = 15$$

$$y_{max} = \frac{N_a \cdot 8D^3 F_{max}}{Gd^4} = 39.51 \text{ mm}$$

$$N_t = 10 \text{ total turns}$$

$$L_s = d(N_t + 1) = 32$$

$$(L_{ocr}) = L_s + (1 + 0.15)y_{max} = 77.43$$

Using these equations, we determined the important factors such as spring rate k , the maximum applicable force on the spring F_{max} , maximum spring displacement, maximum shear stress, and the static factor of safety (FOS) against failure.

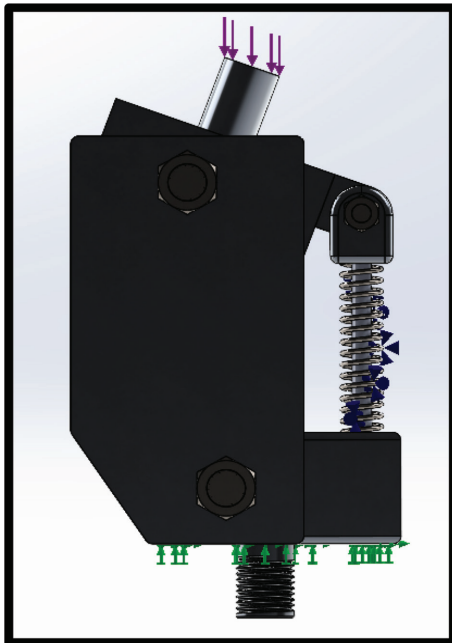


Figure 9: SW external load and reactions. Abbreviation: SW, SOLIDWORKS.

Spring fatigue analysis

Assumption unpeened spring ($S_{sa} = 241$ MPa $S_{sm} = 379$ MPa)

$$F_a = F_m = \frac{F_{max}}{2} = 341.4 \text{ N}$$

$$\tau_a = \tau_m = \frac{8K_B F_a \cdot D}{(\pi d)^3} = 127.46 \text{ MPa}$$

$$S_{ut} = 1999.58 \text{ MPa}$$

$$S_{su} = 0.67S_{ut} = 1339.71 \text{ MPa}$$

$$S_{se} = \frac{S_{sa}}{1 - \left(\frac{S_{sm}}{S_{su}}\right)^2} = 261.96 \text{ MPa}$$

$$n_f = \frac{S_{sa}}{\tau_a} = 1.89$$

Fatigue factor using Goodman: $\frac{1}{n_f} = \frac{\tau_a}{S_{se}} + \frac{\tau_m}{S_{su}} \therefore n_f = 1.719$

The results show that the spring can have infinite lives against fatigue.

INTEGRATION OF SOLIDWORKS SIMULATION AND CALCULATIONS

As we deduced from the calculation, the critical point will happen at gait cycle 55%, knee angle 20°, and $F_z = -3571$ N. So, we studied this point in detail. The simulation results are summarized for each component and are shown in Figures 9-13, respectively.

Knee

So, the FOS of the spring [Shigley et al., 2004] is:

$$n_s = \frac{S_y}{\sigma_{spring \ max}} = \frac{899 \text{ MPa}}{197.8 \text{ MPa}} = 4.55 > 1$$

So, the FOS of the knee is:

$$n_s = \frac{S_y}{\sigma_{kneemax}} = \frac{255 \text{ MPa}}{140 \text{ MPa}} = 1.82 > 1$$

The minimum FOS = 1.5 and it satisfies our specification.

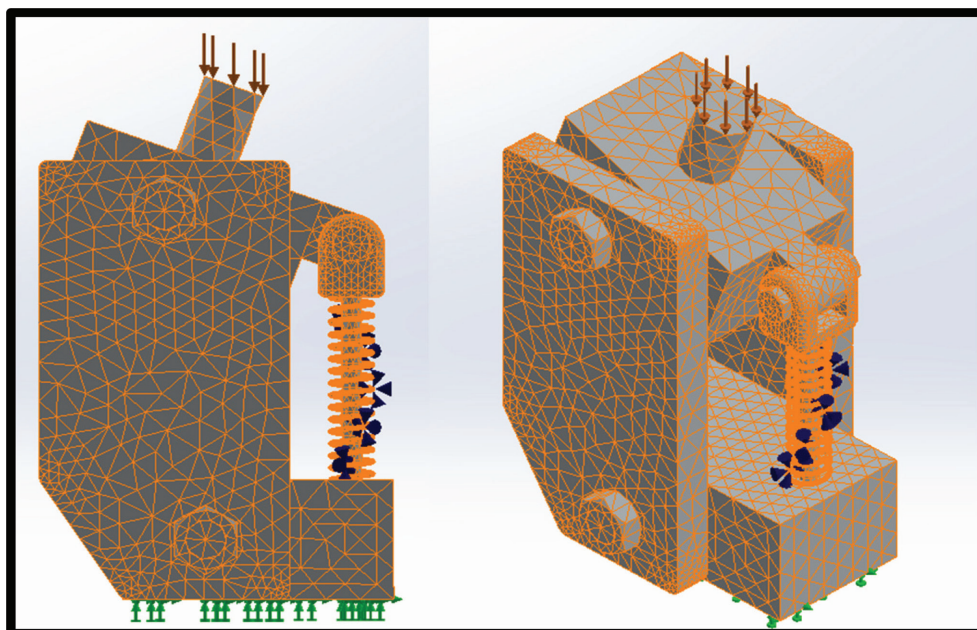


Figure 10: SW knee mesh. Abbreviation: SW, SOLIDWORKS.

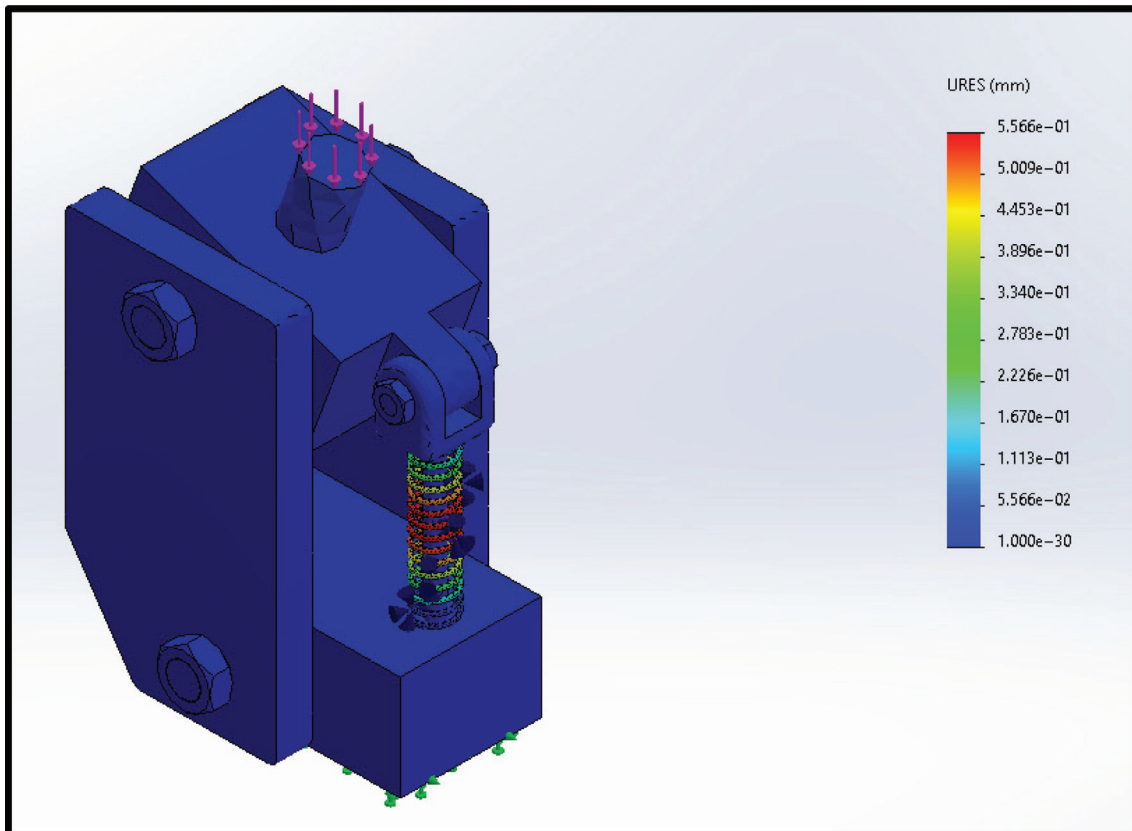


Figure 11: SW knee displacement results. Abbreviation: SW, SOLIDWORKS.

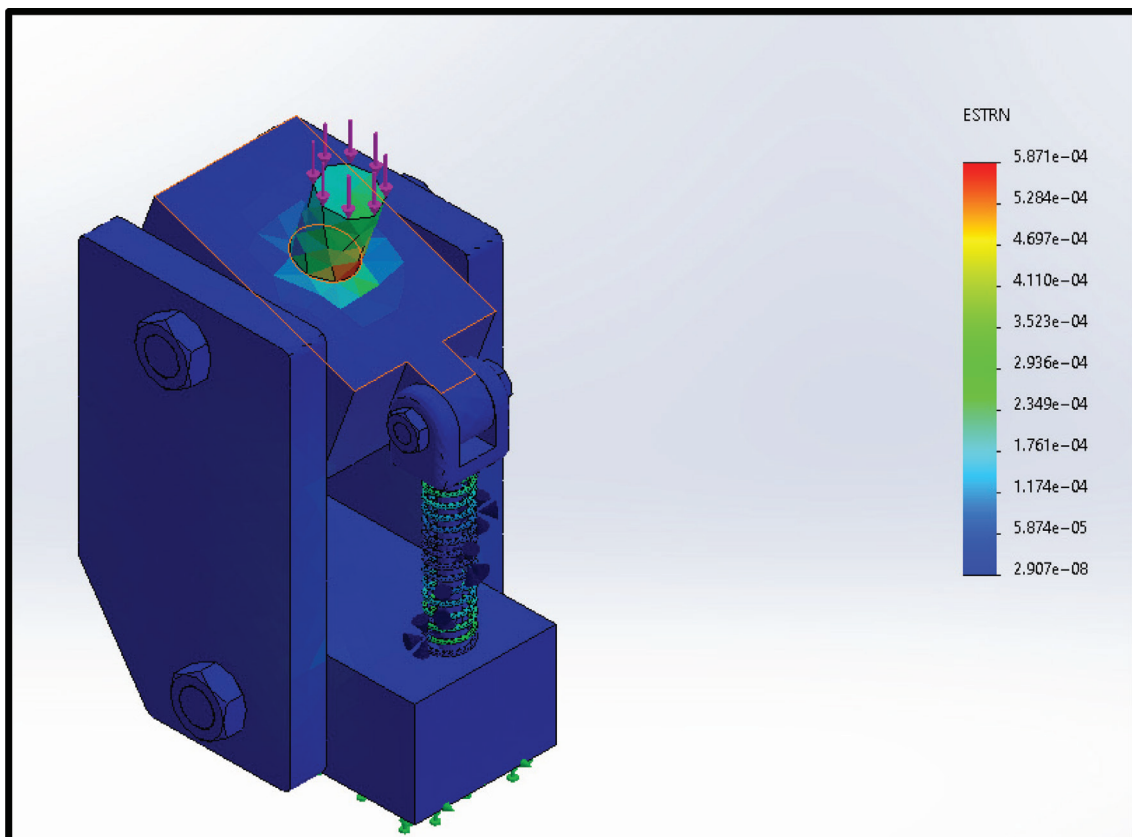


Figure 12: SW knee strain results. Abbreviation: SW, SOLIDWORKS.

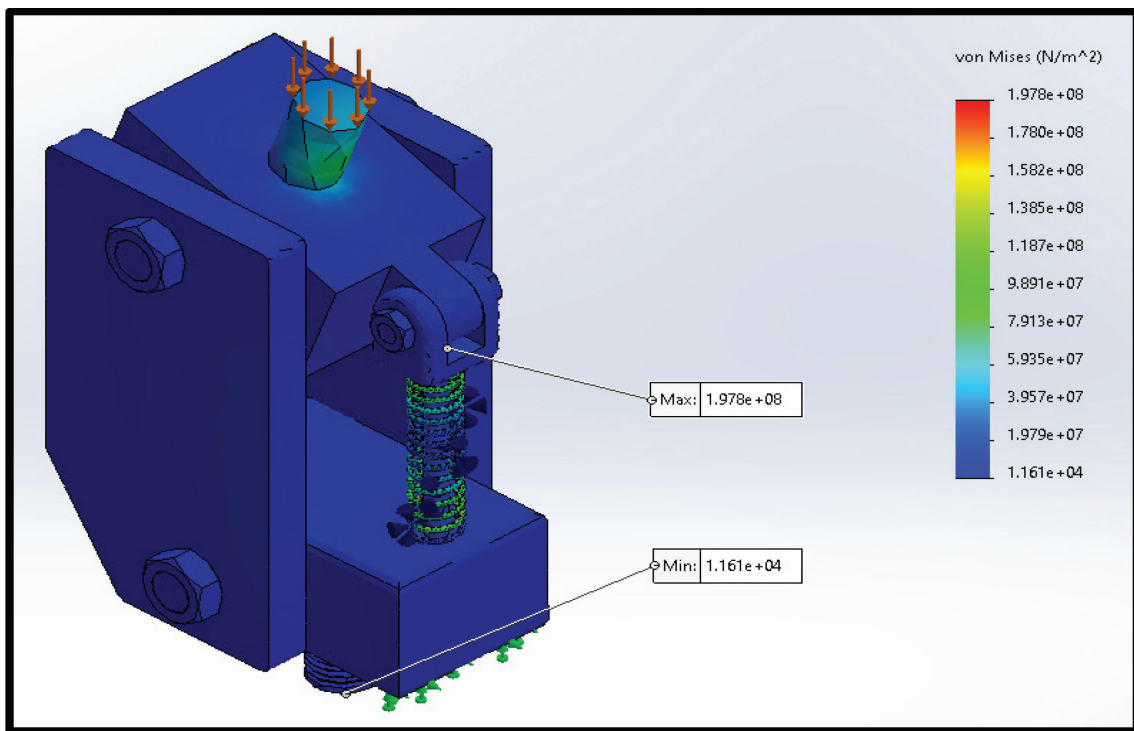


Figure 13: SW knee von Mises stress results. Abbreviation: SW, SOLIDWORKS.

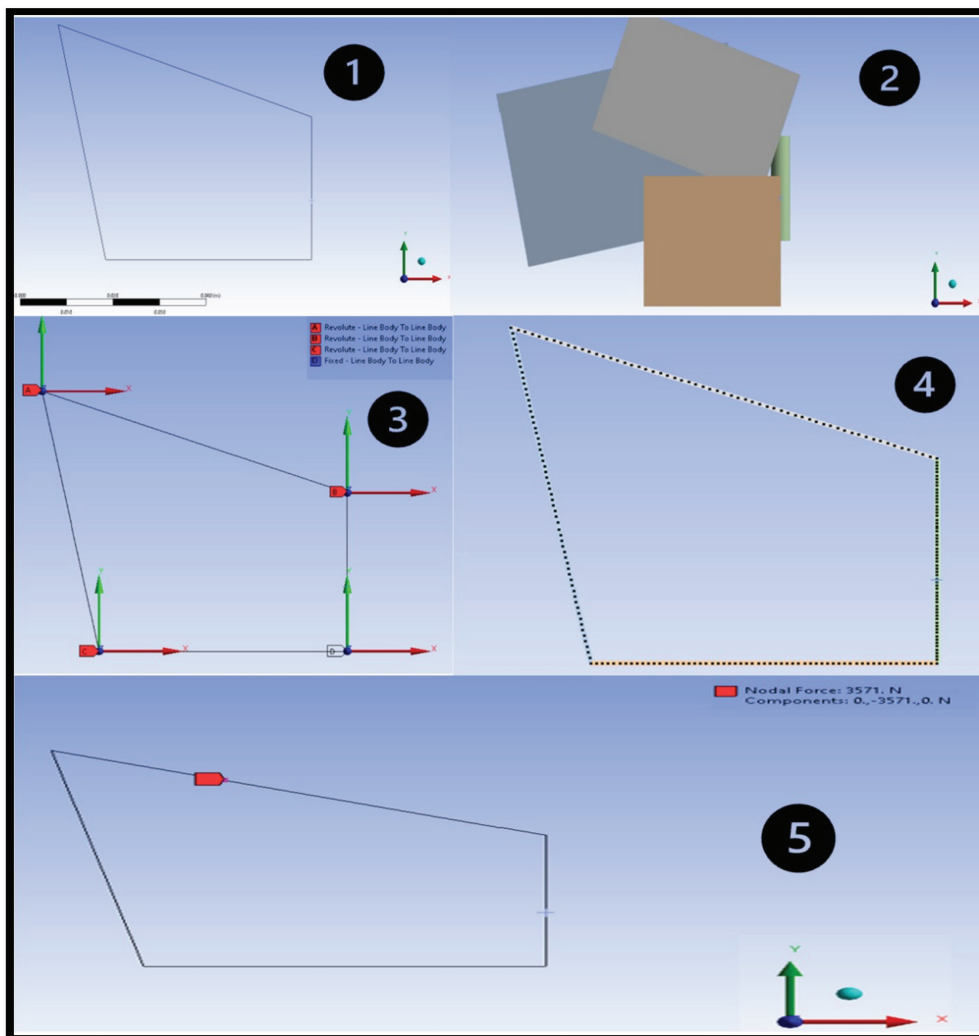


Figure 14: Steps for Ansys simulation and analysis.

Ansysis analysis

Analysis for knee

To study the knee joint in Ansys, we created a simplified two-dimensional (2D) geometry that considers the links between the parts with the cross-section area of each component.

Figure 14 presents the typical steps involved in Ansys simulations. Step (1) represents our geometry by simplifying the parts into 2D links. Step (2) represents the cross section of each part. Step (3) represents the connections between the links and which connection is fixed and which one is revolute. Step (4) represents the default mesh. Step (5) represents the external force acting on the upper connector of the knee.

To obtain a reasonable result, we need to perform a mesh independence study to check if the results are independent of

the mesh or not; this is done by running multiple simulations with different meshes and checking if the results change.

Figure 15 presents the average combined stress on the y-axis with increases in the number of elements on the x-axis. After 400 elements we can see that the line reaches an almost steady state, and changes in the output average combined stress become very small. Therefore, it is reasonable to take 480 elements.

So the FOS [Shigley et al., 2004] of the spring is:

$$n_s = \frac{S_y}{\sigma_{max}} = \frac{899 \text{ MPa}}{200 \text{ MPa}} = 4.495 > 1$$

which is pretty similar to the spring n_s of the SOLIDWORKS (SW) and the theoretical part. And due to the simplification of the body, there was no stress concentration for the thread. Therefore, we are taking into account only the FOS of the spring for this Ansys module.

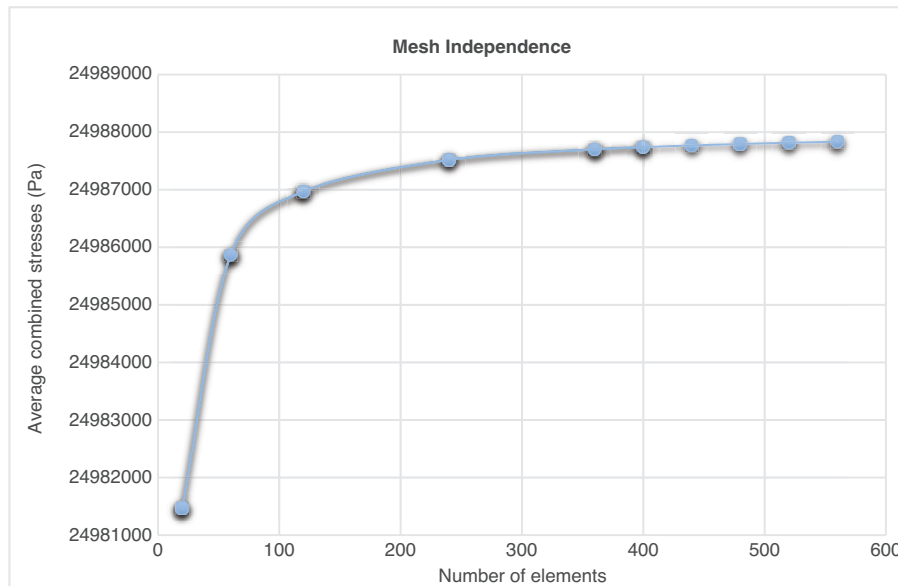


Figure 15: Knee mesh independence chart.

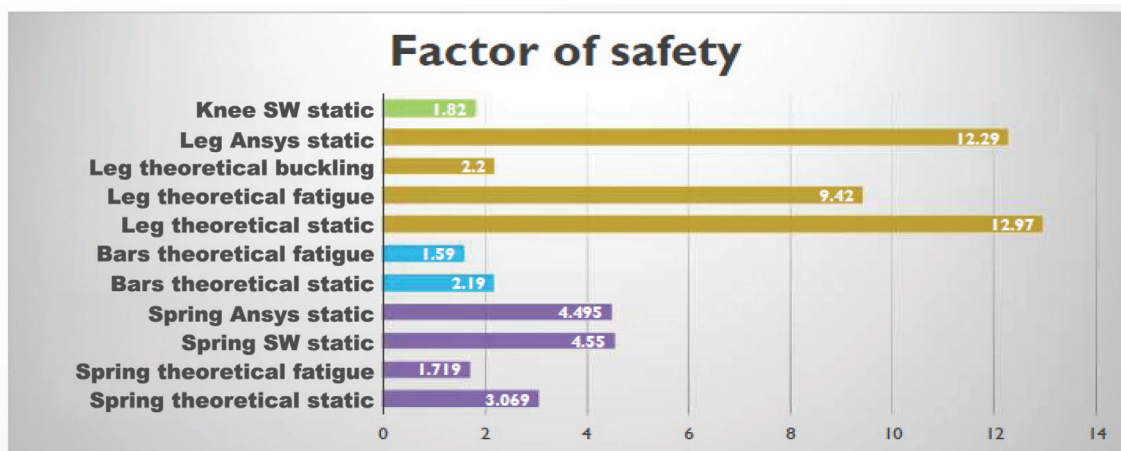


Figure 16: Summary of the factor of safety of each component. Abbreviation: SW, SOLIDWORKS.

Validation of the factor of safety

These static FOSs are high and we can change the material for the static load. But, changing it to a cheaper material would affect the fatigue FOS, which barely met our specification. As our goal was to use a material with high strength and high stiffness, this material is sufficient for our application. As the two bars have the same boundary conditions, external forces, geometries, and material, calculating one of them is enough. Both the FOSs are acceptable according to our constraints. As the FOS is too high for the static and the fatigue, our

material has a specification that exceeds the requirement. Therefore, we can adjust the area, but the height must be the same due to two reasons. One is that the buckling FOS is 2 and it depends on the height. Therefore, changing the height may result in an FOS less than 1.5. The other reason is that the height of the leg depends on the human body dimensions. So, if we change it, there will be no balance and the user will fall. The summary of the FOS for each component of the implant is presented in Figure 16. The complete customized initial design is shown in Figures 17 and 18, respectively.

Customized design of the exoskeleton after manufacturing

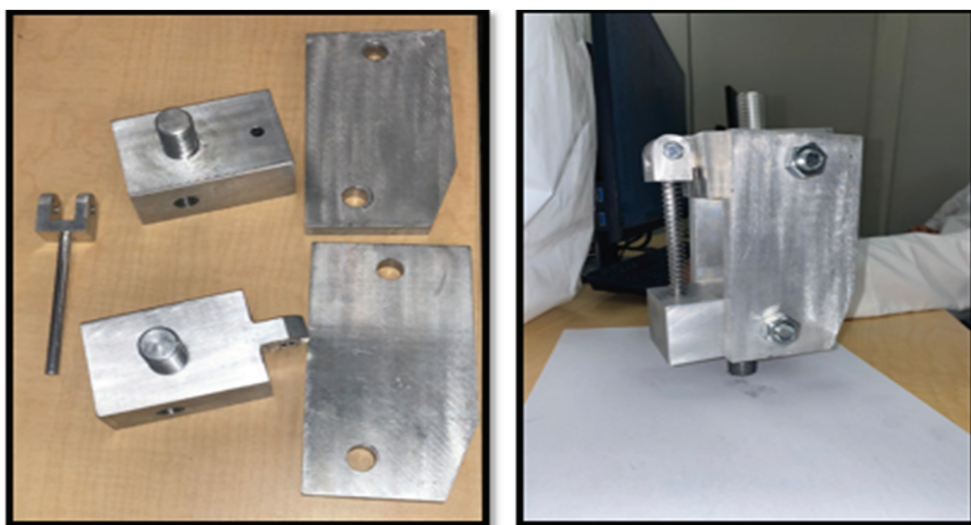


Figure 17: Knee joint prototype.

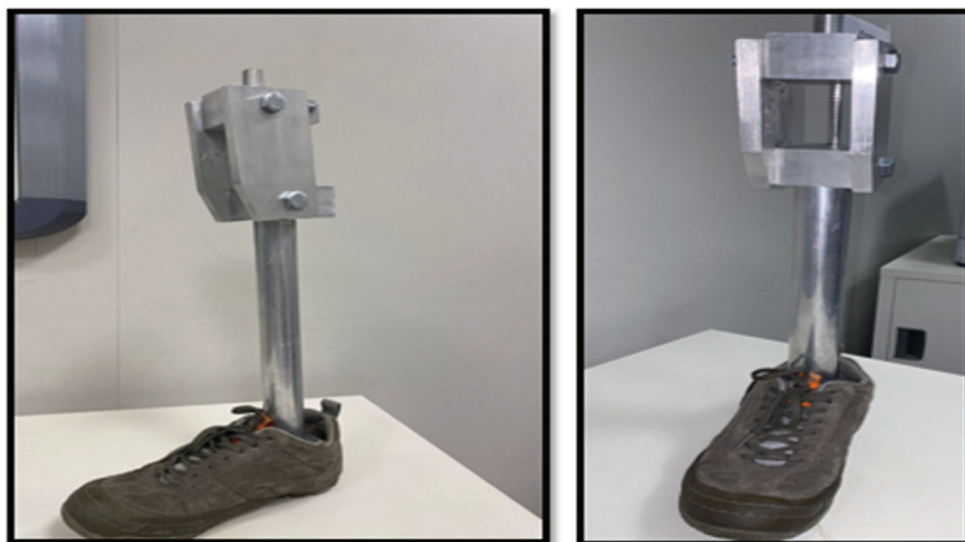


Figure 18: Initial design of the prototype.

COST ANALYSIS

Material cost

The material cost of each part of the assembly as shown in Figures 17 and 18 respectively is estimated to be around 400 SR. The summary of the cost distribution for each component is presented in Table 3. The Al alloy or Ti-based alloys could be promising candidates for the manufacturing of these kind of devices [Ijaz et al.,

2022, 2014, 2016, 2017; Ijaz and Hashmi 2022; Héraud et al., 2023].

CONCLUSION

In the present study, we concluded that our preliminary design could assist in solving problems that our community is facing in terms of the higher cost of artificial implants such as artificial limbs. We tried investigating the reason for

Table 3: Part unit cost vs. receipt cost.

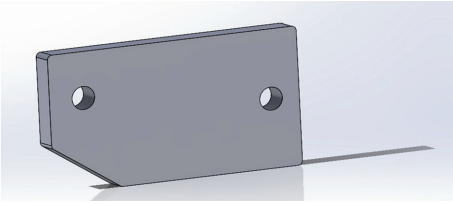
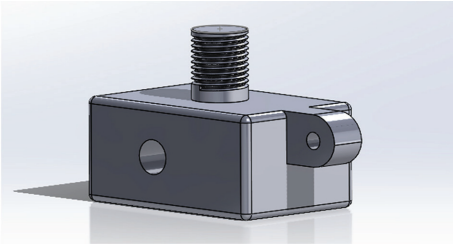
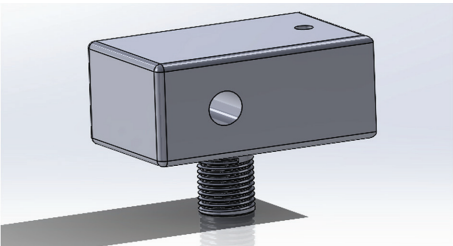
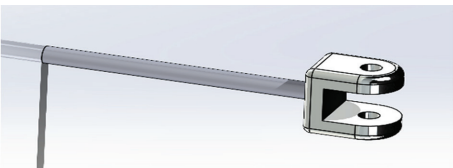
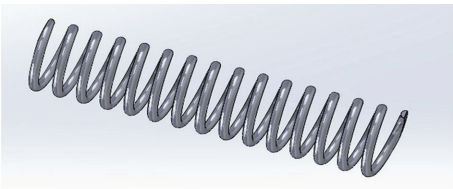
Part	Quantity	Cost
 Plates	2	18.79\$ 70.50 SR
 Upper connector	1	16.38\$ 61.50 SR
 Lower connector	1	17.45\$ 65.50 SR
 Spring connector	1	10.49\$ 40 SR
 Spring	1	3.21\$ 12 SR

Table 3: Continued

Part	Quantity	Cost
 Plates rod	2	6.40\$ 24 SR
 Spring connector rod	1	2.84\$ 11 SR
 Leg rod	1	30.59\$ 115 SR

the higher cost while looking at the existing products on the market, and we figured out that most of the products were designed using chips and microprocessors, which are good but they simultaneously increase the cost. To conclude, a summary of the present study is as follows:

1. We decided to design and fabricate an indigenous cost-effective artificial lower limb, following some constraints and criteria and the weight and rate methodology.
2. We started our project by following the selection methodology until we came up with our final knee joint design which includes a single axis with a spring connecting to a leg rod.
3. Using our knowledge from mechanical engineering, vital mathematical calculations were made to validate the FOS for our designed product.
4. Ansys analysis and SW simulation were utilized to quantify the FOS and make sure it is higher than that we initially considered in the constraints. We proved that from all the methods our device is safe and the FOS is more than 1.5.
5. After finalizing the design, we started choosing the material for the different parts of our product. As this designed

knee implant will be in contact with the human body, we made sure that the material is biocompatible. Thus, we chose aluminum Al-6061 for the other parts of the knee joint and the leg rod.

ACKNOWLEDGMENTS

The authors extend their appreciation to the King Salman Center for Disability Research for providing funding for this work through Research Group number KSRG-2022-033.

FUNDING

The authors are grateful for the financial support provided by the King Salman Center for Disability Research for this work through Research Group number KSRG-2022-033.

REFERENCES

- American Academy of Orthopaedic Surgeons. (1960). *Orthopaedic Appliances Atlas. Volume 2: Artificial Limbs: A Consideration of Aids Employed in the Practice of Orthopaedic Surgery*. JW Edwards, Ann Arbor.
- Andrysek J. (2010). Lower-limb prosthetic technologies in the developing world: a review of literature from 1994–2010. *Prosthet. Orthot. Int.*, 34(4), 378–398.
- Arelekatti V.N.M. (2015). Design of low-cost, fully passive prosthetic knee for persons with transfemoral amputation in India (Doctoral dissertation, Massachusetts Institute of Technology).
- Bergmann G., Bender A., Graichen F., Dymke J., Rohlmann A., Trepczynski A., et al. (2014). Standardized loads acting in knee implants. *PLoS One*, 9(1), e86035.

- Bindawas S.M. and Vennu V. (2018). The national and regional prevalence rates of disability, type, of disability and severity in Saudi Arabia—analysis of 2016 demographic survey data. *Int. J. Environ. Res. Public Health*, 15(3), 419.
- Ebnezar J. (2000). *Textbook of Orthopaedics*. Jaypee Brothers.
- Engstrom B. and Van de Ven C. (Eds.). (1999). *Therapy for Amputees*. Elsevier Health Sciences.
- Farina D. and Aszmann O. (2014). Bionic limbs: clinical reality and academic promises. *Sci. Transl. Med.*, 6(257), 257ps12-257ps12.
- Fliegel O. and Feuer S.G. (1966). Historical development of lower-extremity prostheses. *Arch. Phys. Med. Rehabil.*, 47(5), 275-285.
- Héraud L., Castany P., Ijaz M.F., Gordin D.M. and Gloriant T. (2023). Large-strain functional fatigue properties of superelastic metastable β titanium and NiTi alloys: a comparative study. *J. Alloys Compd.*, 953, 170170.
- Hibbeler R.C. (1994). *Mechanics of Materials*. MacMillan Publishing Company.
- Ijaz M.F. and Hashmi F.H. (2022). Revisiting alloy design of Al-base alloys for potential orthotics and prosthetics applications. *Crystals*, 12(12), 1699.
- Ijaz M.F., Kim H.Y., Hosoda H. and Miyazaki S. (2014). Effect of Sn addition on stress hysteresis and superelastic properties of a Ti–15Nb–3Mo alloy. *Scr. Mater.*, 72, 29-32.
- Ijaz M.F., Laillé D., Héraud L., Gordin D.M., Castany P. and Gloriant T. (2016). Design of a novel superelastic Ti-23Hf-3Mo-4Sn biomedical alloy combining low modulus, high strength and large recovery strain. *Mater. Lett.*, 177, 39-41.
- Ijaz M.F., Dubinskiy S., Zhukova Y., Korobkova A., Pustov Y., Brailovski V., et al. (2017). Novel electrochemical test bench for evaluating the functional fatigue life of biomedical alloys. *JOM*, 69, 1334-1339.
- Ijaz M.F., Alharbi H.F., Bahri Y.A. and Sherif E.S.M. (2022). Alloy design and fabrication of duplex titanium-based alloys by spark plasma sintering for biomedical implant applications. *Materials*, 15(23), 8562.
- Kannenberg A., Zacharias B. and Pröbsting E. (2014). Benefits of microprocessor-controlled prosthetic knees to limited community ambulators: systematic review. *J Rehabil Res Dev.*, 51(10), 1469.
- Lambrecht B.G.A. (2008). *Design of a Hybrid Passive-Active Prosthesis for Above-Knee Amputees*. University of California, Berkeley.
- May B.J. and Lockard M.A. (2011). *Prosthetics & Orthotics in Clinical Practice: A Case Study Approach*. FA Davis, Philadelphia.
- Miller G. (1946). Bibliography of the history of medicine of the United States and Canada—1945. *Bull. Hist. Med.*, 19(5), 536-567.
- Narang Y.S. (2013). Identification of design requirements for a high-performance, low-cost, passive prosthetic knee through user analysis and dynamic simulation (Doctoral dissertation, Massachusetts Institute of Technology).
- Padula P.A. and Friedmann L.W. (1987). Acquired amputation and prostheses before the sixteenth century. *Angiology*, 38(2), 133-141.
- Pirker W. and Katzenschlager R. (2017). Gait disorders in adults and the elderly: a clinical guide. *Wien. Klin. Wochenschr.*, 129(3-4), 81-95.
- Preuss J. (1911). *Biblisch-talmudische Medizin: Beiträge zur Geschichte der Heilkunde und der Kultur überhaupt*. S. Karger, Basel.
- Putti V. (1930). *Historic Artificial Limbs*. Hoeber, New York.
- Rodriguez-Merchan E.C. (2013). Special features of total knee replacement in hemophilia. *Expert Rev. Hematol.*, 6(6), 637-642.
- Shigley J.E., Mischke C.R. and Brown Jr T.H. (2004). *Standard Handbook of Machine Design*. McGraw-Hill Education, New York.